



## RESEARCH REPOSITORY

*This is the author's final version of the work, as accepted for publication following peer review but without the publisher's layout or pagination.  
The definitive version is available at:*

<https://doi.org/10.1016/j.jclepro.2018.11.125>

**Weerasinghe Mohottige, T.N., Kaksonen, A.H., Cheng, K.Y., Sarukkalige, R. and Ginige, M.P. (2018) Kinetics of oxalate degradation in aerated packed-bed biofilm reactors under nitrogen supplemented and deficient conditions. Journal of Cleaner Production**

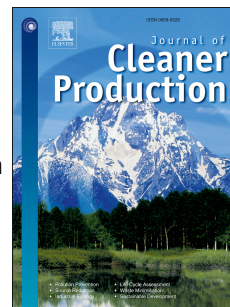
<http://researchrepository.murdoch.edu.au/42623/>

Copyright: © 2018 Elsevier B.V.  
It is posted here for your personal use. No further distribution is permitted

# Accepted Manuscript

Kinetics of oxalate degradation in aerated packed-bed biofilm reactors under nitrogen supplemented and deficient conditions

Tharanga N. Weerasinghe Mohottige, Anna H. Kaksonen, Ka Yu Cheng, Ranjan Sarukkalige, Maneesha P. Ginige



PII: S0959-6526(18)33528-5

DOI: <https://doi.org/10.1016/j.jclepro.2018.11.125>

Reference: JCLP 14884

To appear in: *Journal of Cleaner Production*

Received Date: 30 March 2018

Revised Date: 7 November 2018

Accepted Date: 12 November 2018

Please cite this article as: Weerasinghe Mohottige TN, Kaksonen AH, Cheng KY, Sarukkalige R, Ginige MP, Kinetics of oxalate degradation in aerated packed-bed biofilm reactors under nitrogen supplemented and deficient conditions, *Journal of Cleaner Production* (2018), doi: <https://doi.org/10.1016/j.jclepro.2018.11.125>.

This is a PDF file of an unedited manuscript that has been accepted for publication. As a service to our customers we are providing this early version of the manuscript. The manuscript will undergo copyediting, typesetting, and review of the resulting proof before it is published in its final form. Please note that during the production process errors may be discovered which could affect the content, and all legal disclaimers that apply to the journal pertain.

## **Kinetics of oxalate degradation in aerated packed-bed biofilm reactors under nitrogen supplemented and deficient conditions**

### **Authors**

Tharanga N. Weerasinghe Mohottige<sup>1,2,5</sup>, Anna H. Kaksonen<sup>1,3</sup>, Ka Yu Cheng<sup>1,4</sup>, Ranjan Sarukkalige<sup>2</sup>, Maneesha P. Ginige<sup>1\*</sup>

### **Affiliations**

<sup>1</sup>CSIRO Land and Water, 147 Underwood Avenue, Floreat, WA 6014, Australia

<sup>2</sup>Department of Civil Engineering, Curtin University, Bentley, Western Australia 6102, Australia

<sup>3</sup>School of Pathology and Laboratory Medicine, University of Western Australia, 35 Stirling Highway, Crawley, Western Australia 6009, Australia

<sup>4</sup>School of Engineering and Information Technology, Murdoch University, Western Australia 6150, Australia

<sup>5</sup>School of Computing Engineering and Mathematics, Western Sydney University, Locked Bag 1797, Penrith, NSW 2750

\*Corresponding author. Tel: +61 8 9333 6130; Fax: +61 8 9333 6499.

E-mail address: Maneesha.ginige@csiro.au (Maneesha P. Ginige)

**Abstract**

Destruction of oxalate from alumina-refining process liquor is considered essential for many alumina refineries around the world. Some refineries have embraced the use of aerobic bioreactors as a cost-effective destruction method. These processes are often supplemented with an external nitrogen (N) source to facilitate microbial activity, even though such augmentations are undesirable due to increase of operational costs. Until now, there has also only been little information on oxalate degradation kinetics, although this knowledge is essential to design bioreactor processes. Hence, this study aimed at determining oxalate degradation kinetics in two aerobic packed bed biofilm reactors under both N- supplemented and N-deficient conditions. Michaelis-Menten equation was used to derive kinetic parameters for specific oxalate degradation. The N-deficient culture had a higher affinity ( $K_m$  of 458.4 vs. 541.9 mg/L) towards oxalate and a higher maximum specific oxalate removal rate ( $V_{max}$  of 161.3 vs. 133.3 mg/(h·g biomass)) compared to the N-supplemented culture, suggesting that the N-deficient culture is better suited to remove oxalate. Microbial community analysis also showed differences in the composition of the two cultures. Based on the kinetic parameters derived, a novel two step oxalate removal process was proposed that capitalises on higher specific oxalate removal rates for efficient oxalate destruction from waste streams of alumina industry.

**Key words: bioreactor, kinetics, nitrogen deficient, microbial community, oxalate**

## 1. Introduction

Aluminium is one of the most commercially utilized metals in the world due to its light weight, high strength and excellent corrosion resistance (Meyers, 2004). Pure aluminium does not occur in its metallic form and refining is required to produce aluminium from its mineral ore. Bauxite is the most commonly used aluminium ore and it is refined in Bayer process to produce alumina ( $\text{Al}_2\text{O}_3$ ) (Meyers, 2004; Power et al., 2011). In brief, the major steps of the Bayer process are (1) digestion of bauxite in a hot concentrated caustic solution; (2) recovery of aluminium hydroxide with seeded precipitation at low temperature; and (3) calcination of aluminium hydroxide to produce alumina.

The raw bauxite generally contains organic carbon (0.02 – 0.2% by weight) and a higher percentage is found in Australian bauxite ores (0.2 – 0.3% by weight) as compared to those found in other countries (Hind et al., 1999; Power et al., 2012). The organic impurities are released from the ore during digestion and accumulate in the process liquor due its repeated reuse (Guevara et al., 2017; Power et al., 2012). Among the organic impurities, sodium oxalate severely impacts the productivity and product quality of the Bayer process due to the co-precipitation of oxalate with aluminium hydroxide (Power et al., 2012; Power and Tichbon, 1990). Depending on the plant capacity of an alumina refinery, the daily accumulation of oxalate in spent liquor could be significant. For example, in 2007, an alumina refinery in Western Australia generated 38 - 40 t/d of oxalate while processing 21,000 t/d of bauxite (McSweeney, 2011). To prevent the co-precipitation of oxalate with gibbsite, oxalate concentration in spent liquor is maintained below supersaturation concentrations and a common practise is to maintain a spent liquor oxalate concentration of approximately 2.5 – 2.8 g/L (Barnett et al., 1995; Whelan et al., 2003). The NaOH concentration in spent liquor is approximately 4 M and a direct biological removal of oxalate (~ 40 t/d) from spent liquor would necessitate a reduction of NaOH in spent liquor from 4 M (pH 14.6) down to approximately 0.01 mM (pH 9). A near 99.99975% removal of NaOH from spent liquor is

operationally detrimental to the Bayer process as external addition of NaOH is then needed to increase NaOH concentrations back to 4 M before the effluent could be re-combined with spent liquor. Accordingly, biological removal of oxalate directly from spent liquor is uneconomical. Hence biological oxidation of oxalate is currently practiced by some refineries to destroy oxalate that had been crystallised (oxalate cake) from spent liquor (McKinnon and Baker, 2012).

Prior to the biological destruction of oxalate, liquor burning has been practiced not only remove oxalate but also to recover sodium (as  $\text{Na}_2\text{O}$ ) from crystallised oxalate. Compared to energy costs of liquor burning, biological oxalate degradation is economical and as a consequence alumina refineries are increasingly embracing biological processes to remove oxalate (Chinloy et al., 1993; McKinnon and Baker, 2012). For effective onsite management of oxalate, an efficient biological process that has high volumetric removal rates and a small footprint is highly desirable to minimise capital and operating costs (McKinnon and Baker, 2012).

The bioavailable nitrogen (N) content in crystallised oxalate waste is low, and in current biological oxalate removal processes N requirements are met by adding an external N-source. Hence, the currently used bioreactor processes rely on microbial communities that demand an external N source to oxidise oxalate. Recently, Weerasinghe Mohottige et al. (2018b) for the first time demonstrated the feasibility of using N-fixing haloalkaliphilic bacteria to oxidise oxalate alleviating the need for external dose of N. From an operational point of view the use of N-fixing bacteria without the need to externally supplement N would have environmental and cost benefits for the alumina industry. External N sources, specifically as  $\text{NH}_3$ , are often supplied in excess, to compensate for the possible loss through volatilisation of  $\text{NH}_3$  at high pH. Such operational issues can be avoided with N-deficient systems that utilise N-fixing bacteria (Weerasinghe Mohottige et al., 2018a). Hence the alumina industry could consider utilising N-fixing bacteria specifically if they are demonstrated as comparable or superior in terms of reaction kinetics. However, to date, the

degradation kinetics of oxalate under both N-supplemented and N-deficient conditions has not been explored.

In this study, two aerobic packed bed biofilm reactors (one N-supplemented and the other not supplemented (N-deficient)) were operated for a period of 275 days using a synthetic alkaline, saline oxalate-containing medium. The reactors were operated to mimic a side stream biological oxidation of crystallised oxalate. The Michaelis-Menten model was applied to comparatively assess oxalate degradation kinetic parameters of both cultures to evaluate the suitability of the N-deficient system for industry application. Moreover, the composition of microbial communities in the two reactors were analysed by next generation sequencing to reveal differences in the dominant microbial groups.

## **2. Materials and methods**

The experiments to investigate the kinetic parameters of the oxalate degrading biofilms, were carried out as described below. The laboratory scale bioreactors were operated similar to what is described in Weerasinghe Mohottige et al. (2018a).

### *2.1 Bioreactor set up*

Two identical laboratory-scale packed bed column reactors (Fig. 1) were operated under aerobic conditions. Each packed bed column had an internal diameter and height of 55 mm and 400 mm respectively. The columns were packed with graphite granules (3-5 mm diameter, KAIYU Industrial (HK) limited) to create a bed volume of 600 mL. The mass of the air-dried graphite granules in each reactor was 480 g and once packed, the void volume of the granular column was 210 mL. The granular media in the packed beds were exposed to feed solutions that were continuously aerated in 2 L glass bottles, which were used as solution reservoirs. The feed solutions were recirculated from the reservoirs through the columns in an up-flow direction at a flow rate of

9.6 L/h resulting in a hydraulic retention (HRT) time of 1.3 min in the column reactors. The solution in the reservoirs was changed every 4 h. At the beginning of each 4 h cycle, concentrated stock solutions (carbon and nutrients) were pumped in for 2 min together with deionized water to create a 1.3 L volume of working solution in the reservoirs. To maintain a near saturation level of oxygen in the working solution, compressed air was sparged into the solution reservoirs throughout the entire cycle. At the end of each cycle, the entire volume (i.e. 1.3 L) of the solution reservoirs was decanted, while the graphite granules in the column remained completely submerged. Hence, with retained solution in the column (200 mL), the total volume recirculated in each reactor was 1.5 L.

The reactors were monitored and controlled using data acquisition / control hardware (CompactRio National Instruments, USA) and software (LabVIEW, National Instrument, USA). Online monitoring of dissolved oxygen (DO) and pH were carried out using luminescent DO probes (PDO2, Barben Analyzer Technology, USA) and intermediate junction pH probes (Ionode IJ44, Ionode Pty Ltd, Australia), respectively. In each reactor, two DO probes were used, with one immersed in the liquid of the solution reservoir and the other placed at the outlet of the column reactor. All experiments were carried out at room temperature (~ 23°C).

## 2.2 Synthetic Medium

The working solution for the reactors contained sodium oxalate ( $\text{Na}_2\text{C}_2\text{O}_4$ ) as the carbon source and 25 g/L of NaCl, to simulate salinity of Bayer liquor. The pH of the influent stream was adjusted to 9.0 - 9.5 using 2 M NaOH. The operational pH of 9.0 – 9.5 was chosen based on experimental findings of Weerasinghe Mohottige et al. (2018a). Additionally, the working solution also contained a growth medium, which contained (per L): 125 mg  $\text{NaHCO}_3$ , 51 mg  $\text{MgSO}_4 \cdot 7\text{H}_2\text{O}$ , 15 mg  $\text{CaCl}_2 \cdot 2\text{H}_2\text{O}$ , 20.5 mg  $\text{K}_2\text{HPO}_4 \cdot 3\text{H}_2\text{O}$ , and 1.25 mL of trace element solution. The trace element solution contained (per L): 0.43 g  $\text{ZnSO}_4 \cdot 7\text{H}_2\text{O}$ , 5 g  $\text{FeSO}_4 \cdot 7\text{H}_2\text{O}$ , 0.24 g  $\text{CoCl}_2 \cdot 6\text{H}_2\text{O}$ , 0.99 g  $\text{MnCl}_2 \cdot 4\text{H}_2\text{O}$ , 0.25 g  $\text{CuSO}_4 \cdot 5\text{H}_2\text{O}$ , 0.22 g  $\text{NaMoO}_4 \cdot 2\text{H}_2\text{O}$ , 0.19 g  $\text{NiCl}_2 \cdot 6\text{H}_2\text{O}$ , 0.21 g



$\text{NaSeO}_4 \cdot 10\text{H}_2\text{O}$ , 15 g ethylenediaminetetraacetic acid (EDTA), 0.014 g  $\text{H}_3\text{BO}_3$ , and 0.05 g  $\text{NaWO}_4 \cdot 2\text{H}_2\text{O}$ . This growth media composition is identical to what is reported in Weerasinghe Mohottige et al. (2018a). For the N-supplemented reactor the medium additionally contained 25 mg/L of  $\text{NH}_4\text{Cl}$ . In the medium of the N-deficient reactor,  $\text{NH}_4\text{Cl}$  was replaced with 10 mg/L of yeast extract to supplement unknown micro nutritional requirements of N-fixing bacteria (Gauthier et al., 2000; Sorokin et al., 2008). The nitrogen supplemented and deficient reactors were initially operated with sodium oxalate concentrations of 2.0 g/L and 0.8 g/L, respectively, and the concentrations were later varied for the kinetic experiments.

### 2.3 Microbial inoculum

A sediment sample from Floreat Beach and two soil samples from Perry Lake Reserve (Perth, Western Australia) were used as an inoculum. Oxalic acid is well known to exist in both coastal sediments and around rhizosphere of plants (most plant cells accumulate oxalic acid). Additionally, the microorganisms in coastal sediments are tolerant to saline conditions and soil samples at near vicinity of rhizosphere of native plants contain N-fixing bacteria (Gupta et al., 2014). An equal mass (75 g) of sediment from the three locations were mixed together and placed in two separate 2 L glass bottles. Thereafter, 1.5 L of N-supplemented and N-deficient feed solutions were placed in the respective bottles and 100 mg/L  $\text{Na}_2\text{C}_2\text{O}_4$  was added as a carbon source into each of the bottles. The two bottles were aerated at room temperature for 3 weeks to enrich aerobic oxalate degrading microorganisms. During the enrichment (3 weeks), aeration was interrupted once a week for a period of 1 h to settle suspended solids. Subsequently, the supernatant (1 L) was discarded and replenished with respective fresh feed solutions.

### 2.4 Reactor start up

During the initial 3 weeks, the 2 L bottles were operated without the packed bed column reactors. After 3 weeks of operation, the sediment in each of the bottles were removed upon disturbing the

attached biomass vigorously by shaking. Subsequently, the packed bed columns were connected, and the bottle contents were recirculated through the respective columns.

The 1 d cycle length of the reactors were gradually reduced to 4 h and subsequently  $\text{Na}_2\text{C}_2\text{O}_4$  concentrations in the working solutions were stepwise increased until steady, maximum biofilm activities were achieved. The optimised  $\text{Na}_2\text{C}_2\text{O}_4$  concentrations for the 4 h cycle in the N-supplemented and N-deficient reactors were 2.0 g/L and 0.8 g/L, respectively.

During microbial enrichment and after, cyclic studies were carried out to determine the oxalate removal rates of the bioreactors. Cyclic studies were carried out once every two weeks and the number and the frequency of sampling depended on cycle length. Hourly sampling was carried out once cycle length was reduced to 4 h. During sampling, 3 mL volumes were withdrawn from the 2 L solution reservoirs and were immediately filtered through 0.22  $\mu\text{m}$  pore size syringe filters (Cat. No. SLGN033NK, Merck Pty Ltd, Australia) into 2 mL Eppendorf tubes. The samples were then stored at 4°C until analysed.

### *2.5 Investigating the effect of initial oxalate concentration on oxalate degradation*

After reaching stable reactor performance, the effect of initial oxalate concentration on oxalate degradation kinetic parameters was investigated on both packed bed column reactors. Each initial oxalate concentration was tested over a single 4 h cycle. Between each of the initial oxalate concentrations tested, the biofilm was allowed to recover over 5 normal operational cycles. The initial sodium oxalate concentrations tested with N-supplemented and N-deficient reactors ranged 0.2 - 5 g/L and 0.2 - 4 g/L, respectively. During the kinetic studies, hourly liquid samples (3 mL) were collected, immediately filtered (through 0.22  $\mu\text{m}$  syringe filters (Cat No SLGNO33NK, Merck Millipore, USA)) and stored (at 4°C in 2 mL Eppendorf tubes) for later analysis of oxalate concentrations.

### *2.6 Determination of dry biomass*

The dry mass of biofilm in the packed bed columns was determined by using a known volume (50 mL) of packed granules coated with biomass. Known volumes of graphite media were removed from the reactors and placed together with a known volume (13 mL) of deionized water in 50 mL Falcon tubes. Subsequently, the tubes were placed in an ultra-sonication (Sanophon ultrasonic cleaner - 90 W and 50 Hz) water bath for 3 min to dislodge attached biofilms. The suspensions with dislodged cells were then decanted into new 50 mL Falcon tubes and the graphite media were sonicated once more for 3 min in fresh deionized water. The respective final suspensions were combined and total suspended solids (TSS) and volatile suspended solids (VSS) were measured using methods detailed in the Standard Methods for the Examination of Water and Wastewater (Rice et al., 2012).

### 2.7 Kinetic calculations

The oxalate oxidation rates were normalised to the total dry biomass in the column reactor. Michaelis-Menten equation (Equation 1) and three other graphical representations of enzyme kinetics (Equations 2-4) were used to obtain the kinetic parameters  $V_{\max}$  (maximum initial oxalate removal rate) and  $K_m$  (Michaelis constant - numerically equal to the concentration of substrate that facilitates a half maximal initial oxalate removal rate) for oxalate degradation (Cornish-Bowden, 1995; Kaksonen et al., 2003).  $V$  is the degradation rate,  $[S]$  is the substrate concentration,  $V_{\max}$  is the maximum degradation rate and  $K_m$  is Michaelis-Menten constant.

Michaelis-Menten equation:

$$V = (V_{\max} \times [S]) / (K_m + [S]) \quad (1)$$

Lineweaver-Burk plot:

$$1/V = (K_m/V_{\max}) \times (1/[S]) + (1/V_{\max}) \quad (2)$$

Hanes Plot:

$$[S]/V = (K_m/V_{\max}) + (1/V_{\max}) \times [S] \quad (3)$$

Eadie-Hofstee plot:

$$V = V_{\max} - K_m \times (V/[S]) \quad (4)$$

### 2.8 Oxygen uptake rate calculation

The oxygen uptake rates (OUR) of biofilm were determined in accordance to equation 5.

$$OUR = \frac{DO_{in} - DO_{out}}{HRT \times \text{mass of dry biomass}} \times \text{Reactor liquid volume} \quad (5)$$

Where  $DO_{in}$  and  $DO_{out}$  are influent and effluent dissolved oxygen concentrations (mg  $O_2$  /L) of column reactor, HRT (h) is the hydraulic retention time of the column reactor, the reactor liquid volume (L) is the total liquid volume of the reactor and mass of dry biomass (g) is the amount of biomass attached onto the graphite media.

### 2.9 Assessment of N deficient conditions

The nitrogen deficient reactor did not receive any form of nitrogen other than 10 mg/L of yeast extract throughout the experimental period. The use of yeast extract is common specifically to supplement essential nutrient requirements for the growth of nitrogen fixing bacteria (Gauthier et al., 2000; Sorokin et al., 2008). To confirm the absence of inorganic nitrogen in the reactor, liquid samples collected from the influent and effluent of the reactor were analysed for soluble nitrate ( $NO_3^-$ ), nitrite ( $NO_2^-$ ) and ammonium ( $NH_4^+$ ) using a Dionex ICS-3000 reagent free ion chromatography (RFIC) system.

### 2.10 Chemical analysis

Oxalate and other anion (i.e. formate and acetate) concentrations were analysed using the RFIC system, which was fitted with an IonPac® AS18  $4 \times 250$  mm column. Potassium hydroxide was the eluent for anion separation at a flow rate of 1 mL/min. The eluent concentration was 12-45 mM from 0-5 min, 45 mM from 5-8 min, 45-60 mM from 8-10 min and 60-12 mM from 10-13 min.

$\text{NH}_4^+\text{-N}$  was measured with the same RFIC but with a IonPac® CG16, CS16, 5 mm column using 30 mM methanesulfonic acid eluent with a flow rate of 1 mL/min for 29 min. The temperature of the two columns were maintained at 30°C. Suppressed conductivity was used as the detection signal (ASRS ULTRA II 4 mm, 150 mA, AutoSuppression® recycle mode).

### 2.11 Microbial Analysis

The biofilm coated granules (15 mL) were separately collected from each packed bed column reactor into two 50 mL centrifuge tubes for DNA extraction. Sampling for microbial community analysis was carried out after 3 weeks of reactor start-up (Samples no. NS21D and ND21D from N-supplemented and N-deficient reactors, respectively) and during optimisation of N-supplemented (Samples NS83D, NS141D and NS221D on days 83, 141 and 221, respectively) and N-deficient reactor (Samples ND225D, ND253D and ND280D on days 225, 253 and 280, respectively) operation. Letters ND and NS in sample names refer to the nitrogen deficient and nitrogen supplemented reactor respectively, the numerical digits refer to number of days from start-up of the reactors and the character D represents days. On collection of the granules into the 50 mL centrifuge tubes, deionized water (20 mL) was added and the tubes were sonicated for 2 min in a Sanophon ultrasonic water bath (90 W, 50 Hz) to detach the biomass. The liquid containing the dislodged biomass were collected in fresh 50 mL centrifuge tubes and the granules were sonicated once more with another equal volume of fresh deionized water. Thereafter the two sonication liquid samples were combined and the biomass in each of the samples were harvested by centrifugation (at 6000 g for 5 min). The supernatants were subsequently decanted and the pelleted biomass was used for DNA extraction.

#### 2.11.1 DNA extraction

DNA was extracted from 250  $\mu\text{L}$  of pelleted biomass using the Power Soil DNA isolation kit (MO BIO laboratories, USA) following manufacturer's instructions. The extracted DNA was quantified

using a Qubit fluorometer and stored at -20°C prior to delivery to the School of Pathology and Laboratory Medicine, University of Western Australia for 454 sequencing.

### 2.11.2 Microbial community analysis

The 454 sequencing was carried out as described in (Nagel et al., 2016). In brief, microbial 16S rRNA genes were amplified from 1 ng aliquots of the extracted DNA using V4/5 primers (515F: GTGCCAGCMGCCGCGGTAA and 806R: GGACTACHVGGGTWTCTAAT). A mixture of gene-specific primers and gene-specific primers tagged with Ion Torrent-specific sequencing adaptors and barcodes were used. The tagged and untagged primers were mixed at a ratio of 90:10. Using this method, the amplification of all samples was achieved with 18–20 cycles, minimising primer-dimer formation. The amplification was confirmed by agarose gel electrophoresis, and the PCR products were quantified using fluorometry. Up to 100 amplicons were diluted to equal concentrations and adjusted to a final concentration of 60 pM. Templated Ion Sphere Particles (ISP) were then generated and loaded onto sequencing chips using an Ion Chef (ThermoFisher Scientific) and samples were sequenced on a PGM semiconductor sequencer (ThermoFisher Scientific) for 650 cycles using a 400 bp sequencing kit typically yielding a modal read length of 309 bp. Data collection and read trimming/filtering were performed using TorrentSuite 5.0.

Post sequence analysis was carried out using an open source software package QIIME (Quantitative Insights Into Microbial Ecology) (Caporaso et al., 2010). The fasta, qual and mapping files were analysed using downstream computational pipelines of QIIME. The chimeric reads were identified and filtered using USEARCH and an unaligned reference Greengenes database (gg\_13\_5.fasta obtained from [http://greengenes.secondgenome.com/downloads/database/13\\_5](http://greengenes.secondgenome.com/downloads/database/13_5)). Subsequently operational taxonomic units (OTUs) were assigned at 97% sequence similarity using the same reference database file from Greengenes. For each OTU picked, a representative sequence was assigned and a final taxonomic assignment was carried out using the RDP classifier version 2.2 (Wang et al., 2007) with reference to the same Greengenes database. The unprocessed DNA

sequences of this study were deposited (accession numbers SRR5982975, SRR5982976 to SRR5982982) in NCBI's Sequence Read Archive (SRA) (Meyer et al., 2008).

### 3. Results and Discussion

Both N-supplemented and N-deficient reactors showed a stable removal of oxalate after approximately 200 d of operation. Possible intermediate compounds such as acetate and formate that can result from aerobic oxidation (Lung et al., 1994) and/or anaerobic fermentation (Weerasinghe Mohottige et al., 2018a) of oxalate were not detected in this study. Hence, oxalate removal was assumed a result of complete mineralisation to CO<sub>2</sub>. Regular monitoring of inorganic nitrogenous species in N-deficient reactor revealed no detectable concentration of NO<sub>3</sub><sup>-</sup>-N, NO<sub>2</sub><sup>-</sup>-N and NH<sub>4</sub><sup>+</sup>-N in both the influent and effluent of the reactor. In N-supplemented reactor, although no NO<sub>3</sub><sup>-</sup>-N and NO<sub>2</sub><sup>-</sup>-N were detected, an NH<sub>4</sub><sup>+</sup>-N concentration of approximately 6 ± 3 mg/L and < 0.8 mg/L was detected in the influent and effluent, respectively. The low NH<sub>4</sub><sup>+</sup>-N concentration in the effluent was likely due to volatilisation of NH<sub>3</sub> at high pH and usage by microorganisms for growth and cell maintenance. The N demand of the N-deficient reactor, on the other hand, was likely fulfilled with atmospheric fixation of N<sub>2</sub>.

After 3 weeks of enrichment, the oxalate removal rates of N-supplemented and N-deficient reactors were 34 mg/(L·h) and 1 mg/(L·h), respectively. The oxalate removal rate of the N-supplemented reactor showed a linear increase (from 34 to 364 mg/(L·h) (R<sup>2</sup> = 0.98)) during the optimisation of reactor operation. In contrast, a much slower linear increase of oxalate removal was recorded for N-deficient reactor and during stable operation of reactor, a steady removal rate of 187 mg/(L·h) was achieved. A typical cyclic study, of N-supplemented and N-deficient reactors (Fig. 2) showed a linear decrease of oxalate over time. During the 3.5 h reaction time, alongside removal of oxalate, a

gradual decrease of pH was noted (a reduction of pH from 9.5 to 8.7 and 9.3 to 8.8 in N-supplemented and N-deficient reactors, respectively) in both reactors. Biological degradation of oxalate generates carbonate, and this resulted in a decrease of pH in the reactors (Fig. 2). Unlike pH, the oxygen uptake rate (OUR) of both reactors remained steady (285 mg/(L·h) and 140 mg/(L·h) in N-supplemented and in N-deficient reactors, respectively) throughout the cycle and the OUR only decreased (to 75 mg/(L·h) and 70 mg/(L·h) in N-supplemented and in N-deficient reactors respectively (Data not shown)) on complete exhaustion of oxalate in both reactors. The reduced OUR values represent endogenous respiration rates of the reactors.

### 3.1 Oxalate degradation kinetics

In this study, a sequencing batch mode of operation was used with both N-supplemented and N-deficient reactors. Sequencing batch reactors are highly beneficial specifically when enforcing strict hydraulic boundaries. However, continuous flow reactors are desired specifically to minimise complexities of operation. In order to conceptualise oxalate removal in continuous flow reactors with these two cultures, kinetic parameters were derived for oxalate degradation using Michaelis-Menten equation for both N-supplemented and N-deficient reactors.

Specific oxalate removal rates for different initial in-reactor oxalate concentrations are shown in Fig. 3A (Figure S1 reflects data used to derive initial specific oxalate removal rates). There was no decline of specific oxalate removal rates, when initial in-reactor concentrations were increased and hence a substrate level inhibition was not evident with in-reactor concentrations tested in this study. Since the relationship between the independent variable, initial oxalate concentration (S), and the dependent variable, initial specific rate of oxalate removal (V) was curvilinear, the estimation of the two parameters ( $V_{\max}$  and  $K_m$ ) were derived using three linear transformations (Lineweaver-Burk plot, Hanes Plot and Eadie-Hofstee plot) of equation 1. Equations 2, 3, and 4 are all variants of Equation 1 and theoretically all three linear transformations should result in identical values for



$V_{\max}$  and  $K_m$ . However, this is never the case simply due to measurement errors of  $V$  and  $S$  (Dowd and Riggs, 1965).

The  $V_{\max}$  and  $K_m$  values derived in this study using the three linear transformations of Michaelis-Menten equation are summarised in Table 1, which also reports the coefficient of determination ( $R^2$ ) for each of the three linear transformations (Figs 3B – D). Both Lineweaver-Burk and Hanes Plots showed a good fit to the data ( $R^2$  values of  $> 0.92$ ), while a poor fit was noted with Eadie-Hofstee plot ( $R^2$  values of  $< 0.87$ ). The  $R^2$  values reflect measurement errors associated with  $V$  and  $S$  and a low  $R^2$  value with Eadie-Hofstee plot suggested that  $V_{\max}$  and  $K_m$  should not be derived using Eadie-Hofstee plot. Although a good fit can be observed with Lineweaver-Burk plot, it also has been sometimes reported to give deceptively good fits according to Dowd et al. (1965). Based on Hanes plot, which gave the highest  $R^2$  value of  $>0.97$ , the  $V_{\max}$  values of the N-supplemented and N-deficient reactors were 133.3 and 161.3 mg/(h·g biomass), respectively and the corresponding  $K_m$  values were 541.9 and 458.4 mg/L, respectively. Hence, in this study,  $V_{\max}$  and  $K_m$  values derived using the Hanes Plot ( $R^2$  values of  $> 0.97$ ) were used in subsequent calculations. From an operational perspective, the  $K_m$  value is of significance as it reflects the affinity of the culture to the substrate (oxalate). A low  $K_m$  value indicates that the culture has a high affinity towards a substrate and vice versa. Accordingly, the N-deficient culture has a higher affinity towards oxalate and consequently can reach closer to its maximum oxalate removal rates at lower oxalate concentrations. To achieve a similar specific removal rate of oxalate, the N-supplemented reactor required exposure to a higher in-reactor oxalate concentration. Hence, when a low concentration of oxalate is desired in bioreactor effluent, the N-deficient culture is likely to facilitate it with a shorter HRT. A shorter HRT on the other hand helps to reduce reactor footprint, and capital and operating costs.

### *3.2 A side stream two-step continuous biological treatment process for efficient removal of oxalate*

According to Michaelis-Menten kinetics, higher oxalate removal rates can only be achieved with higher in-reactor oxalate concentrations. Accordingly, a two-stage biological treatment process (Fig. 4) is proposed to make use of the higher degradation rates at higher oxalate concentrations to achieve an efficient removal of oxalate. When considering saturation concentrations, the maximum in-reactor oxalate concentration that could be maintained is approximately 3 g/L (Hiralal et al., 1994). At such an in-reactor concentration of oxalate, a specific oxalate removal rate of 112.9 or 139.9 mg/(h·g biomass) can be facilitated with either N-supplemented or N-deficient reactor biomass, respectively (Table 2). The second reactor (polish-up reactor) could then be operated to polish up bulk of the remaining oxalate to reduce the effluent concentration to 0.4 g/L for the effluent to be discharged into alkaline lakes in the refinery (Tilbury, 2003). At this effluent concentration the oxalate degradation rates would be 56.6 and 75.2 mg/(h·g biomass) in the N-supplemented and N-deficient reactor, respectively (Table 2).

If 40 t/d of oxalate is to be biologically destructed using an influent oxalate concentration of 100 g/L, the required HRTs for the two-stage bioreactor would be 1.43 and 1.57 d for N-supplemented and N-deficient systems, respectively. In comparison, the corresponding single stage systems would require HRTs of 2.52 and 2.87 d for N-supplemented and N-deficient systems respectively (Table 2). The differences in HRT would translate to required total reactor volumes to be 1626 m<sup>3</sup> and 1648 m<sup>3</sup> for the two stage systems operated under N-supplemented and N-deficient conditions, respectively, while the corresponding one-stage systems would require volumes of 3060 m<sup>3</sup> and 2904 m<sup>3</sup>, respectively. Hence the use of the two-stage system would allow the total reactor volume to be decreased by nearly 55% (from approximately one Olympic size swimming pool to half a pool) while still allowing equally good effluent quality. This would considerably reduce the footprint of biological oxalate destruction, and likely decrease capital and operating costs (Table 2). A future study should comparatively examine the operation of single- and a two-stage N-supplemented and deficient oxalate removing bioreactors to systematically examine the aforementioned benefits of a two-stage biological process.

### *3.3 Kinetic differences reflect the differences in microbial community composition*

Despite the approximate equal reactor volume requirements for N-supplemented and N-deficient reactors to treat 40 t/d of oxalate, the biomass density of N-supplemented reactor was approximately 1.3 times higher than that of N-deficient reactor. The difference in specific removal rates was likely due to the differences in microbial community composition between the N-deficient and N-supplemented reactors.

Both N-supplemented and N-deficient reactors were inoculated with the same source of inoculum. The microbial community changes of both reactors were examined from start-up until stable reactor performance using 454 pyrosequencing of 16S rRNA genes. Rarefaction curves of all samples sequenced indicated that sequencing depth was adequate to capture bacterial diversity present in the samples (Figure S2). The Principal coordinate analysis (PCoA) of unweighted Unifrac distances (which measures similarity of microbial communities based on phylogenetic diversity), showed clustering of microorganisms according to the availability of N in the reactors (Figure S3). A similar clustering was noted with the unweighted pair group method with arithmetic mean (UPGMA) tree (Fig. 5). The samples collected from both reactors after 3 weeks of inoculation clustered together, indicating a greater phylogenetic similarity between microbial communities of the N-supplemented and N-deficient reactors than during later stages of operation when each reactor appeared to have microbial communities that were uniquely different to one another (Fig 5 and Figure S3). When examining the single cluster formed by samples of N-deficient reactor (Fig. 5), there was no major change in the composition between days 253 and 280, suggesting the reactor achieved a stable community. In contrast, the microbial community composition of the N-supplemented reactor changed somewhat more between days 141 and 221 suggesting that the reactor was yet to reach stability.

Although the PCoA and UPGMA analysis showed similarity between the microbial community compositions of samples collected on 21 d from N-supplemented and N-deficient reactors, the dominant taxa in these samples differed considerably (Fig. 6A). The dominant taxa in the N-

supplemented and N-deficient reactors are shown in Fig. 6A. Once stable reactor performance was achieved, approximately 90% of sequences in N-supplemented reactor were associated with bacterial classes Alphaproteobacteria (~53%), Betaproteobacteria (~24%), Gammaproteobacteria (~9%) and Bacilli (~4%). In contrast in the N-deficient reactor 78% of sequences were evenly spread across bacterial classes Alphaproteobacteria (~23%), Gammaproteobacteria (~23%), Betaproteobacteria (~18%) and Cytophaga (~14%).

When the abundance of microbial taxa was examined at a genus level, *Paracoccus* and *Azoarcus* of bacterial classes Alphaproteobacteria and Betaproteobacteria, respectively appeared dominant in both reactors (Fig. 7A). During the study period, the relative abundance of *Paracoccus* and *Azoarcus* increased in the N-supplemented reactor, whereas the increase of genus *Paracoccus* in the N-deficient reactor was lower. Compared to the N-deficient reactor, the dominance of *Paracoccus* in N-supplemented reactor suggested a possible dependence of this genus on a ready source of nitrogen. The *Paracoccus* spp. associated with roots of *Amorphophallus* plants have been demonstrated to be capable of oxidising oxalate (Anbazhagan et al., 2007). Compared to *Paracoccus*, genus *Azoarcus* showed a similar level of dominance in both reactors. Genus *Azoarcus* is known for its nitrogen-fixing capabilities specifically associated with plant roots in soil (Reinholdhurek et al., 1993) and some species of the genus can oxidise oxalate (Mechichi et al., 2002) and McSweeney et al. (2011) demonstrated the abundance of *Azoarcus* in a pilot and in a full-scale moving bed bioreactor operated for biological oxalate destruction. Genus *Alkaliphilus* of family *Clostridiaceae* and an unknown genus of family *Rhodobacteraceae* also showed an increase in abundance during the operation of the N-supplemented reactor (Fig. 7B). Similar increasing trends were observed for bacterial taxon KSA1 of family *Balneolaceae* and unknown bacterial genera of families *Rhodobacteraceae*, *Flammeovirgaceae* and *Marinicellaceae* of the N-deficient reactor (Fig. 7C).

### 3.4 Implications of this study

This study for the first time reveals beneficial aspects of using a N-deficient culture to remove oxalate present in alumina refinery waste. Compared to the N-supplemented culture, the N-deficient culture had a higher affinity towards oxalate and was able to degrade oxalate at a higher maximum specific rate. The non-requirement of an external N source also makes N-deficient cultures a more attractive alternative for the alumina industry to biologically remove oxalate from its alumina waste. The beneficial aspects associated may include a reduction of operational costs and footprint of the treatment unit. Based on the kinetic data derived from this study, a two-stage treatment process with a reduced reactor footprint is proposed (Fig. 4). In contrast to a one-stage process, the two-stage process demands a substantially smaller (43%) reactor footprint, as the first reactor of the two-stage process is operated at the higher specific oxalate removal rate of the culture. A higher specific oxalate removal rate is only achievable with maintenance of a higher in-reactor oxalate concentration. Hence, in the two-stage process the main reactor was designed to maintain a higher in-reactor oxalate concentration. Finally, to achieve the desired effluent quality a polish up reactor is required, in which the target effluent oxalate concentration (0.4 g/L) only facilitates a lower (46%) specific oxalate removal rate compared to the main reactor. However, because of the reduced oxalate loading, even with a reduced specific oxalate removal rate, the footprint required for the polish up reactor is only minor (~94% less) compared to what is required for the master reactor. This implies that the proposed process may substantially reduce the overall HRT required for oxalate removal (45% less than the conventional one-stage process), allowing the alumina industry to treat its oxalate waste more efficiently.

#### 4. Conclusions

The kinetics of oxalate degradation under N-supplemented and N-deficient conditions was comparatively examined to explore the feasibility of facilitating side-stream removal of oxalate from alumina refineries without external nitrogen supplementation. The N-deficient culture had a

higher affinity (a low  $K_m$  of 458.4 vs. 541.9 mg/L) towards oxalate and a higher oxalate removal rate ( $V_{max}$  of 161.3 vs. 133.3 mg/(h·g biomass)) than the N-supplemented culture. This suggested that the N-deficient culture was better suited for oxalate destruction. Even with a lower biomass density, the footprint of the N-deficient bioreactor was similar to the N-supplemented bioreactor due to the differences in the reaction kinetics of the two cultures. Molecular analysis of the microbial communities also showed differences in the two cultures, although bacterial genera *Azoarcus* and *Paracoccus* which are known to harbour oxalate degraders were detected in both cultures. To capitalise on higher specific oxalate removal rates, a two-step treatment process was proposed to destruct oxalate waste generated by alumina industry. The two-step process would achieve a low oxalate concentration in the effluent with a smaller reactor footprint than a single-reactor process.

### **Acknowledgements**

The funding from CSIRO Mineral Resources, CSIRO Land and Water, and Curtin University Postgraduate Scholarship (CUPS) is gratefully acknowledged. The authors thank Dr Yosephine Gumulya and Dr Qing Hu from CSIRO Land and Water and CSIRO Mineral Resources, respectively for valuable comments on the manuscript.

## Reference

- Anbazhagan, K., Raja, C.E., Selvam, G.S., 2007. Oxalotrophic *Paracoccus alcaliphilus* isolated from *Amorphophallus* sp rhizoplane. World J. Microbiol. Biotechnol. 23(11), 1529-1535.
- Barnett, N.W., Bowser, T.A., Russell, R.A., 1995. Determination of oxalate in alumina process liquors by ion chromatography with post column chemiluminescence detection. Anal. Proc. 32(2), 57-59.
- Caporaso, J.G., Kuczynski, J., Stombaugh, J., Bittinger, K., Bushman, F.D., Costello, E.K., Fierer, N., Pena, A.G., Goodrich, J.K., Gordon, J.I., Huttley, G.A., Kelley, S.T., Knights, D., Koenig, J.E., Ley, R.E., Lozupone, C.A., McDonald, D., Muegge, B.D., Pirrung, M., Reeder, J., Sevinsky, J.R., Tumbaugh, P.J., Walters, W.A., Widmann, J., Yatsunenko, T., Zaneveld, J., Knight, R., 2010. QIIME allows analysis of high-throughput community sequencing data. Nat. Meth. 7(5), 335-336.
- Chinloy, D.R., Doucet, J., McKenzie, M.A., The, K.I., 1993. Processes for the alkaline biodegradation of organic impurities. Google Patents.
- Cornish-Bowden, A., 1995. Fundamentals of enzyme kinetics, Revised ed. Portland Press Ltd, London.
- Dowd, J.E., Riggs, D.S., 1965. A comparison of estimates of Michaelis-Menten kinetic constants from various linear transformations. J. Biol. Chem. 240(2), 863-&.
- Gauthier, F., Neufeld, J.D., Driscoll, B.T., Archibald, F.S., 2000. Coliform bacteria and nitrogen fixation in pulp and paper mill effluent treatment systems. Appl. Environ. Microbiol. 66(12), 5155-5160.
- Guevara, H.P.R., Ballesteros, F.C., Vilando, A.C., De Luna, M.D.G., Lu, M.C., 2017. Recovery of oxalate from bauxite wastewater using fluidized-bed homogeneous granulation process. J. Cleaner Prod. 154, 130-138.
- Gupta, V.V.S.R., Kroker, S.J., Hicks, M., Davoren, C.W., Descheemaeker, K., Llewellyn, R., 2014. Nitrogen cycling in summer active perennial grass systems in South Australia: non-symbiotic nitrogen fixation. Crop Pasture Sci. 65(10), 1044-1056.

- Hind, A.R., Bhargava, S.K., Grocott, S.C., 1999. The surface chemistry of Bayer process solids: A review. *Colloid Surface A*. 146(1-3), 359-374.
- Hiralal, I.D.K., Holewijn, J.E., Moretto, K., 1994. Critical oxalate concentration (COC) determination in Bayer plant liquors using a turbidity method. *Light Met.*, 53-57.
- Kaksonen, A.H., Franzmann, P.D., Puhakka, J.A., 2003. Performance and ethanol oxidation kinetics of a sulfate-reducing fluidized-bed reactor treating acidic metal-containing wastewater. *Biodegradation* 14(3), 207-217.
- Lung, H.Y., Baetz, A.L., Peck, A.B., 1994. Molecular cloning, DNA sequence, and gene expression of the oxalyl-coenzyme A decarboxylase gene, *oxc*, from the bacterium *Oxalobacter formigenes*. *J. Bacteriol.* 176(8), 2468-2472.
- McKinnon, A.J., Baker, C.L., 2012. Process for the destruction of organics in a Bayer process stream. Patent US2014/0051153 A1, 28.
- McSweeney, N.J., 2011. The microbiology of oxalate degradation in bioreactors treating Bayer liquor organic wastes, School of biomedical, biomolecular chemical sciences, Microbiology and Immunology. University of Western Australia, Australia, pp. 53-58.
- McSweeney, N.J., Tilbury, A.L., Nyeboer, H.J., McKinnon, A.J., Sutton, D.C., Franzmann, P.D., Kaksonen, A.H., 2011. Molecular characterisation of the microbial community of a full-scale bioreactor treating Bayer liquor organic waste. *Miner. Eng.* 24(11), 1094-1099.
- Mechichi, T., Stackebrandt, E., Gad'on, N., Fuchs, G., 2002. Phylogenetic and metabolic diversity of bacteria degrading aromatic compounds under denitrifying conditions, and description of *Thauera phenylacetica* sp nov., *Thauera aminoaromatica* sp nov., and *Azoarcus buckelii* sp nov. *Arch. Microbiol.* 178(1), 26-35.
- Meyer, F., Paarmann, D., D'Souza, M., Olson, R., Glass, E.M., Kubal, M., Paczian, T., Rodriguez, A., Stevens, R., Wilke, A., Wilkening, J., Edwards, R.A., 2008. The metagenomics RAST server - a public resource for the automatic phylogenetic and functional analysis of metagenomes. *BMC Bioinform.* 9, 386.



- Meyers, R.A.E., 2004. Encyclopedia of physical science and technology: Third edition, Materials Chapter : Aluminum. Academic Press, New York, pp. 495-518.
- Nagel, R., Traub, R.J., Allock, R.J.N., Kwan, M.M.S., Bielefeldt-Ohmann, H., 2016. Comparison of faecal microbiota in Blastocystis-positive and Blastocystis-negative irritable bowel syndrome patients. *Microbiome* 4:47.
- Power, G., Loh, J.S.C., Niemela, K., 2011. Organic compounds in the processing of lateritic bauxites to alumina Addendum to Part 1: Origins and chemistry of organics in the Bayer process. *Hydrometallurgy* 108(1-2), 149-151.
- Power, G., Loh, J.S.C., Vernon, C., 2012. Organic compounds in the processing of lateritic bauxites to alumina Part 2: Effects of organics in the Bayer process. *Hydrometallurgy* 127, 125-149.
- Power, G., Tichbon, W., 1990. Sodium oxalate in the Bayer process: Its origin and effects, Second International Alumina Quality Workshop. Perth, pp. 99-115.
- Reinholdhurek, B., Hurek, T., Gillis, M., Hoste, B., Vancanneyt, M., Kersters, K., Deley, J., 1993. *Azoarcus* gen. nov., nitrogen-fixing Proteobacteria associated with roots of Kallar grass (*Leptochloa fusca* (L.) kunth), and description of 2 species, *Azoarcus-indigenus* sp. nov. and *Azoarcus communis* sp. nov. . *Int. J. Syst. Bacteriol.* 43(3), 574-584.
- Rice, E.W., Bridgewater, L., American Public Health Association., American Water Works Association., Water Environment Federation., 2012. Standard methods for the examination of water and wastewater, 22 ed. American Public Health Association, Washington, D.C.
- Sorokin, I.D., Kravchenko, I.K., Doroshenko, E.V., Boulygina, E.S., Zadorina, E.V., Tourova, T.P., Sorokin, D.Y., 2008. Haloalkaliphilic diazotrophs in soda solonchak soils. *FEMS Microbiol. Ecol.* 65(3), 425-433.
- Tilbury, A., 2003. Biodegradation of Bayer organics in residue disposal systems, Department of Chemistry. University of Western Australia.

Wang, Q., Garrity, G.M., Tiedje, J.M., Cole, J.R., 2007. Naive Bayesian classifier for rapid assignment of rRNA sequences into the new bacterial taxonomy. *Appl. Environ. Microbiol.* 73(16), 5261-5267.

Weerasinghe Mohottige, T.N., Cheng, K.Y., Kaksonen, A.H., Sarukkalige, R., Ginige, M.P., 2018a. Influences of pH and organic carbon on oxalate removal by alkaliphilic biofilms acclimatized to nitrogen-deficient and supplemented conditions. *J. Cleaner Prod.* 187, 699-707.

Weerasinghe Mohottige, T.N., Cheng, K.Y., Kaksonen, A.H., Sarukkalige, R., Ginige, M.P., 2018b. Oxalate degradation by alkaliphilic biofilms acclimatized to nitrogen-supplemented and nitrogen-deficient conditions. *J. Chem. Technol. Biotechnol.* 93(3), 744-753.

Whelan, T.J., Ellis, A., Kannangara, G.S.K., Marshall, C.P., Smeulders, D., Wilson, M.A., 2003. Macromolecules in the Bayer process. *Rev. Chem. Eng.* 19(5), 431-472.

Table 1. Michaelis-Menten constants ( $K_m$ ) and maximum specific oxalate degradation rates ( $V_{max}$ ) for N-supplemented and N-deficient reactor systems obtained with three different linearization approaches.

Linearization Approach	$K_m$ (mg/L)		$V_{max}$ (mg/(h·g biomass))		$R^2$	
	N-supplemented	N-deficient	N-supplemented	N-deficient	N-supplemented	N-deficient
Lineweaver-Burk plot	366.6	262.9	114.9	129.9	0.9237	0.9748
Hanes Plot	541.9	458.4	133.3	161.3	0.9747	0.9845
Eadie-Hofstee plot	386.2	326.3	120.8	144.6	0.7918	0.8721

Table 2. Design parameters for one stage and two stage bioreactor processes assuming oxalate generation of 40 t/d and influent oxalate concentration of 100 g/L

Parameter	Unit	One-stage process	Two-stage process	
			Main reactor	Polish-up reactor
Oxalate Loading	t/d	40	40	1.2
Influent oxalate concentration	g/L	100	100	3
Influent flow rate	m <sup>3</sup> /d	400	400	400
<b>N-supplemented process</b>				
Maximum specific Oxalate removal rate ( $V_{max}$ )	g/(h·g biomass)	0.133	0.133	0.133
Michaelis-Menten constants ( $K_m$ )	g/L	0.542	0.542	0.542
Effluent [Oxalate] - [S]	g/L	0.40	3.00	0.40
Specific oxalate removal rate ( $V$ ) <sup>a</sup>	g/(h·g biomass)	0.057	0.113	0.057
Biomass density per media volume (based on lab reactor)	g biomass/m <sup>3</sup>	9622	9622	9622
Oxalate degradation rate (based on media volume)	g/(d·m <sup>3</sup> )	13071	26072	13071
Media to liquid volume ratio (based on lab reactor)		3.0	3.0	3.0
HRT	d	2.52	1.23	0.07
Effective reactor liquid volume	m <sup>3</sup>	1,008	492	26
Biological media volume (Reactor Volume)	m <sup>3</sup>	3060	1534	92
Size equivalent to an Olympic size swimming pool (2500 m <sup>3</sup> )		1.22	0.61	0.04
<b>N-deficient process</b>				
Maximum specific Oxalate removal rate ( $V_{max}$ )	g/(h·g biomass)	0.161	0.161	0.161
Michaelis-Menten constants ( $K_m$ )	g/L	0.4584	0.4584	0.4584
Effluent [Oxalate] - [S]	g/L	0.40	3.00	0.40
Specific Oxalate removal rate ( $V$ ) <sup>a</sup>	g/(h·g biomass)	0.075	0.140	0.075
Biomass density per media volume (based on lab reactor)	g biomass/m <sup>3</sup>	7632	7632	7632
Oxalate degradation rate (based on media volume)	g/(d·m <sup>3</sup> )	13768	25629	13768
Media to liquid volume ratio (based on lab reactor)		2.5	2.5	2.5
HRT	d	2.87	1.50	0.07
Effective reactor liquid volume	m <sup>3</sup>	1,147	600	30
Biological media volume (Reactor Volume)	m <sup>3</sup>	2905	1561	87
Size equivalent to an Olympic size swimming pool (2500 m <sup>3</sup> )		1.16	0.62	0.03

<sup>a</sup> Calculated based on Hanes plot linearization for the in-reactor oxalate concentration (i.e. effluent oxalate concentration)

**Figure captions**

Fig. 1. A schematic diagram of the laboratory-scale aerobic packed bed bioreactor.

Fig. 2. Profiles of in-reactor oxalate concentration, oxygen uptake rate (OUR) and pH during a 3.5 h aerobic reactor operation.

Fig. 3. [A] Effect of initial oxalate concentration ( $S$ ) on specific oxalate degradation rate ( $V$ ) in N-supplemented and N-deficient reactors. Linearization of results with [B] Lineweaver-Burk plot; [C] Hanes plot, and [D] Eadie-Hofstee plot.

Fig. 4. A schematic diagram of a side stream continuous biological oxalate removal process.

Fig. 5. Similarity analysis (at 97% sequences similarity) of microbial communities in N-supplemented and N-deficient reactors 3 weeks after inoculation and during stable operation based on unweighted Unifrac - Unweighted pair group method with arithmetic mean (UPGMA) cluster analysis. The values on branches show the similarity of the microbial communities.

Fig. 6. [A] Relative abundance of microbial class (having a  $\geq 3\%$  abundance) observed in N-supplemented and N-deficient reactors. [B] Specific oxalate removal rates of the two reactors at the time sample collection for microbial community analysis.

Fig. 7. Change of abundance of microbial genera during the operation of N-supplemented and N-deficient reactors. [A] A comparison of relative abundance of genera *Azoarcus* and *Paracoccus*; [B] Other bacterial genera that showed a positive increase of abundance - N-supplemented reactor; [C] Other bacterial genera that showed a positive increase of abundance - N-deficient reactor.

Fig. 1.

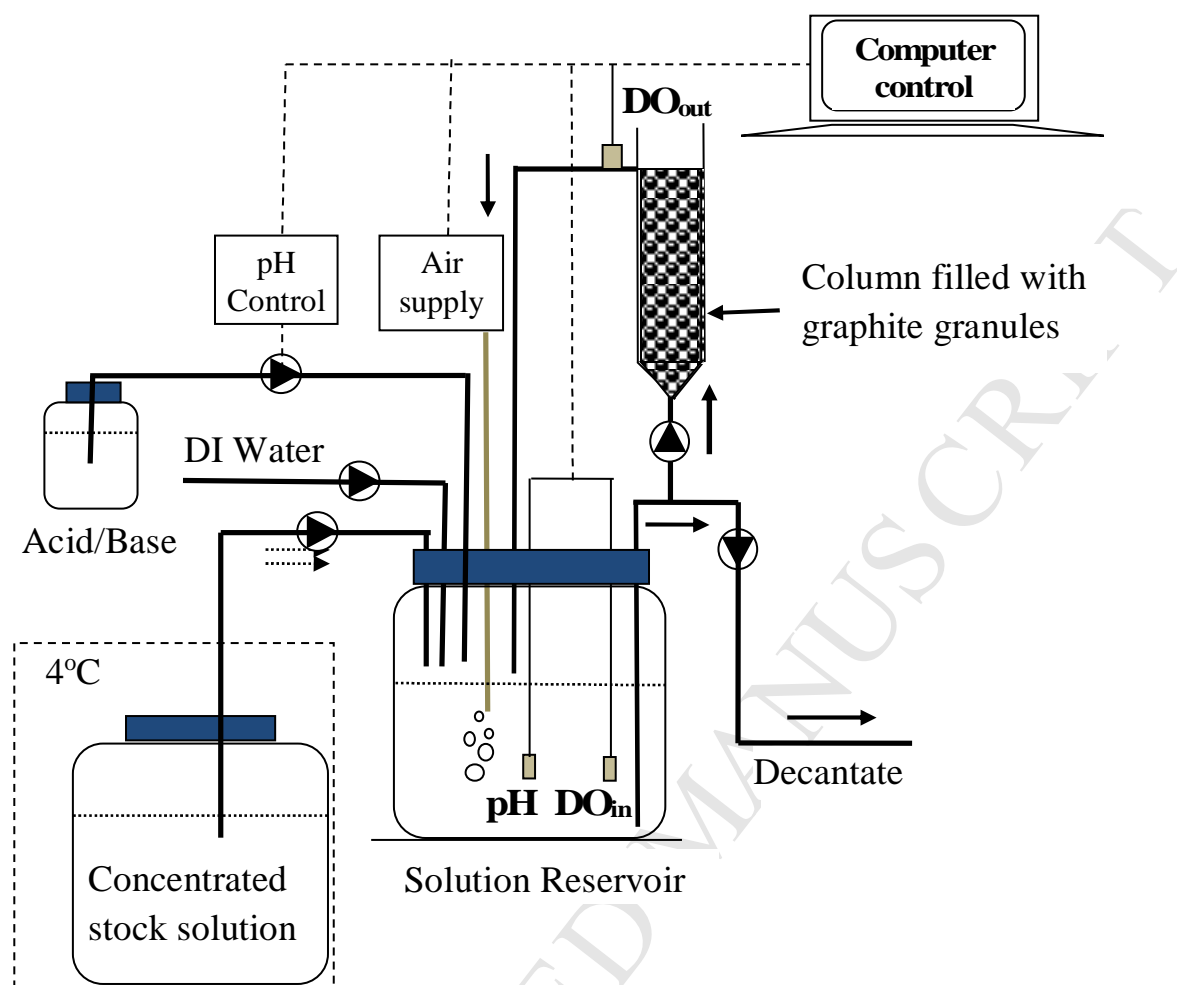


Fig. 2.

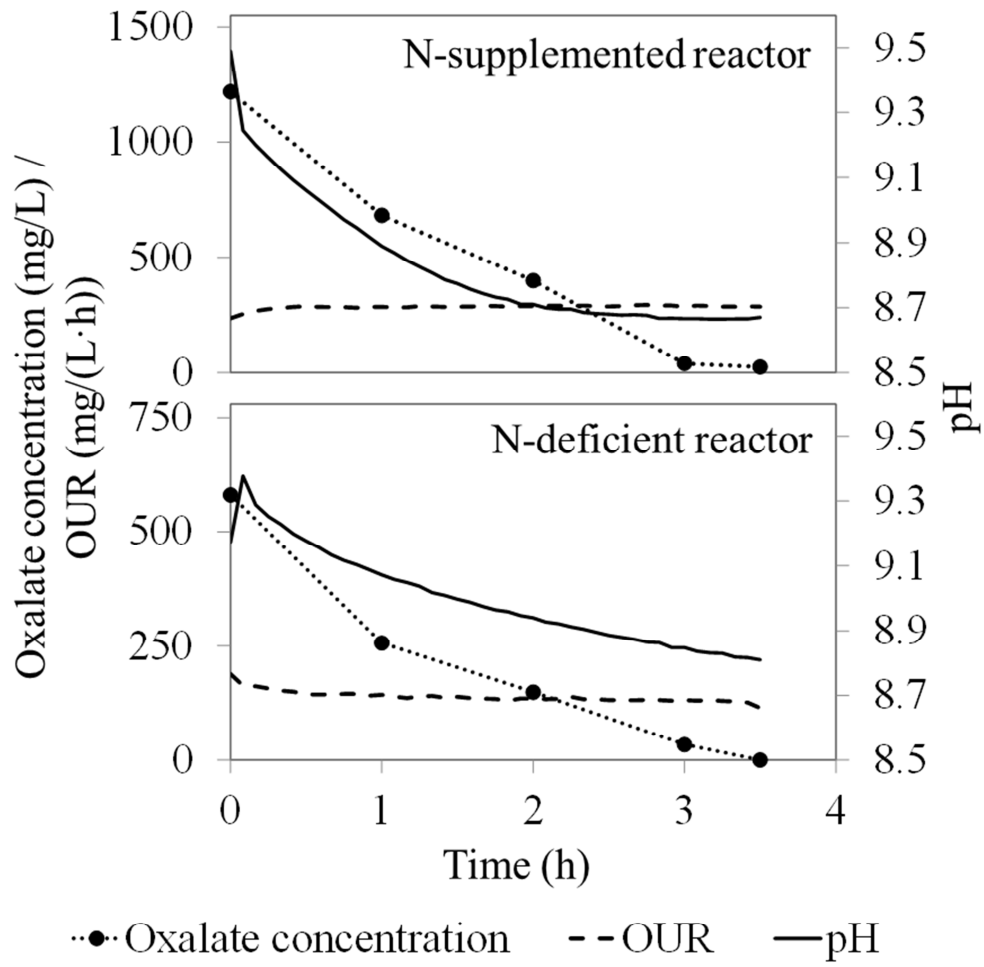


Fig. 3.

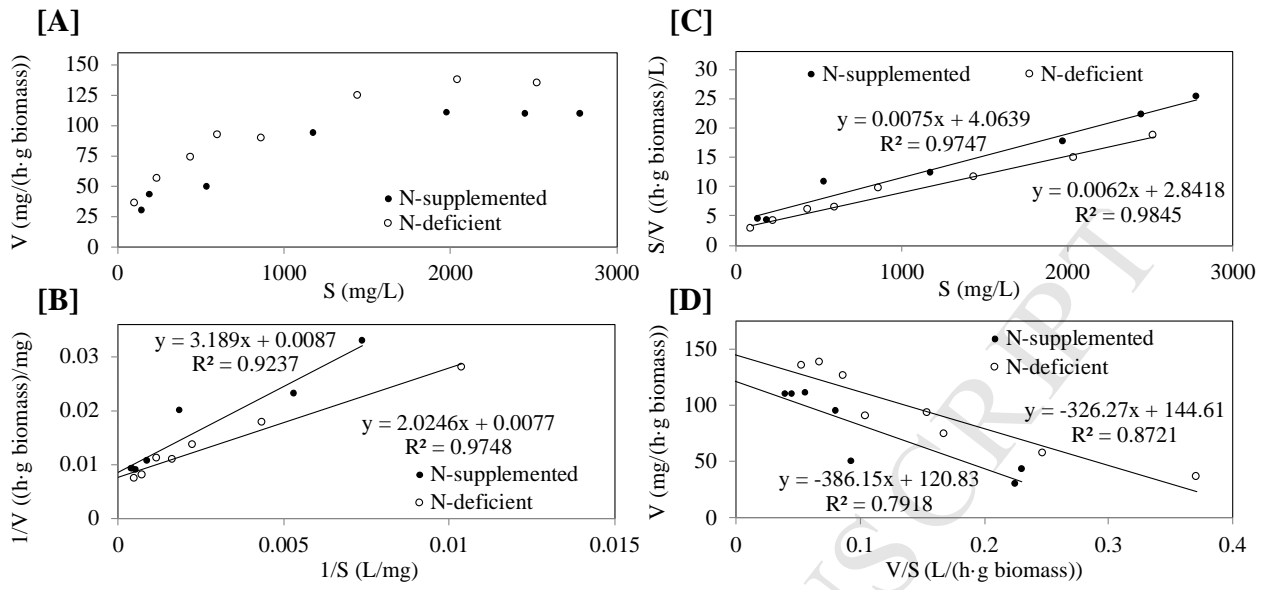




Fig. 4.

Two stage process	Main reactor	Polish-up reactor	Total HRT (d)
	Oxalate removal rate (mg/(h·g biomass))		
N-supplemented	113	57	1.43
N-deficient	140	75	1.57

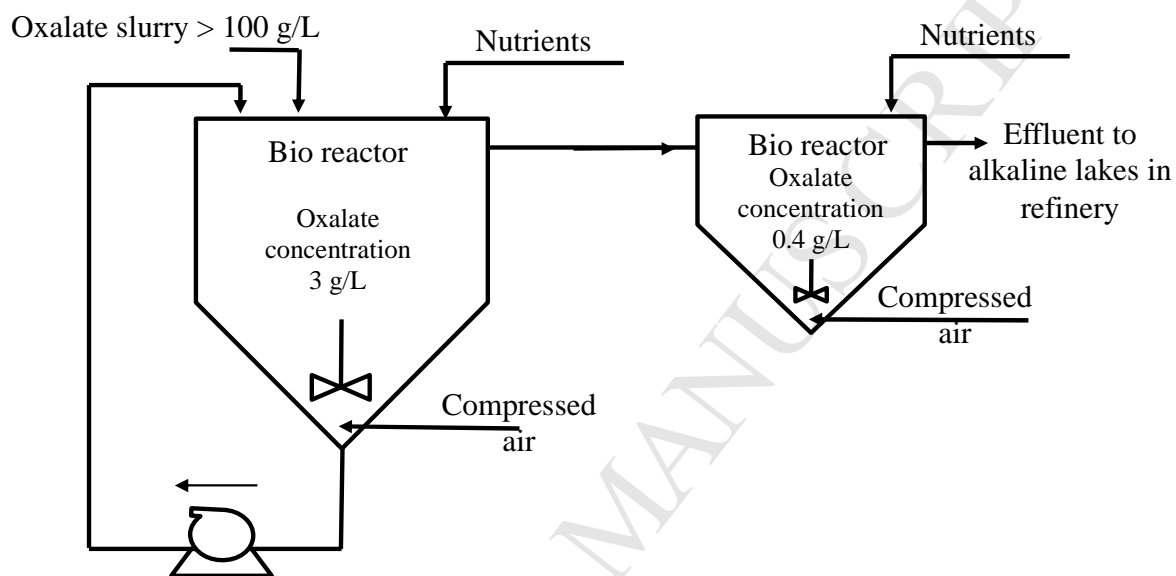


Fig. 5.

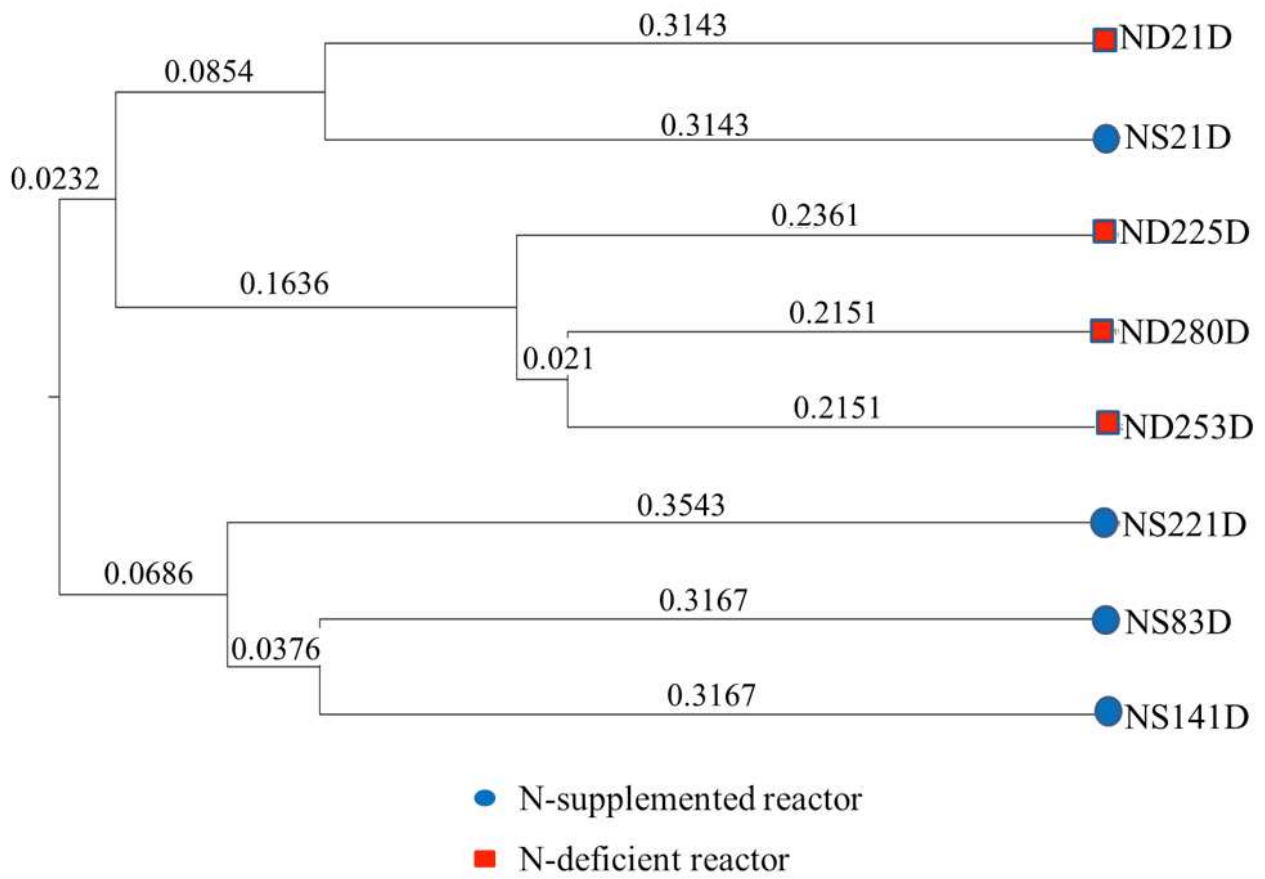


Fig. 6.

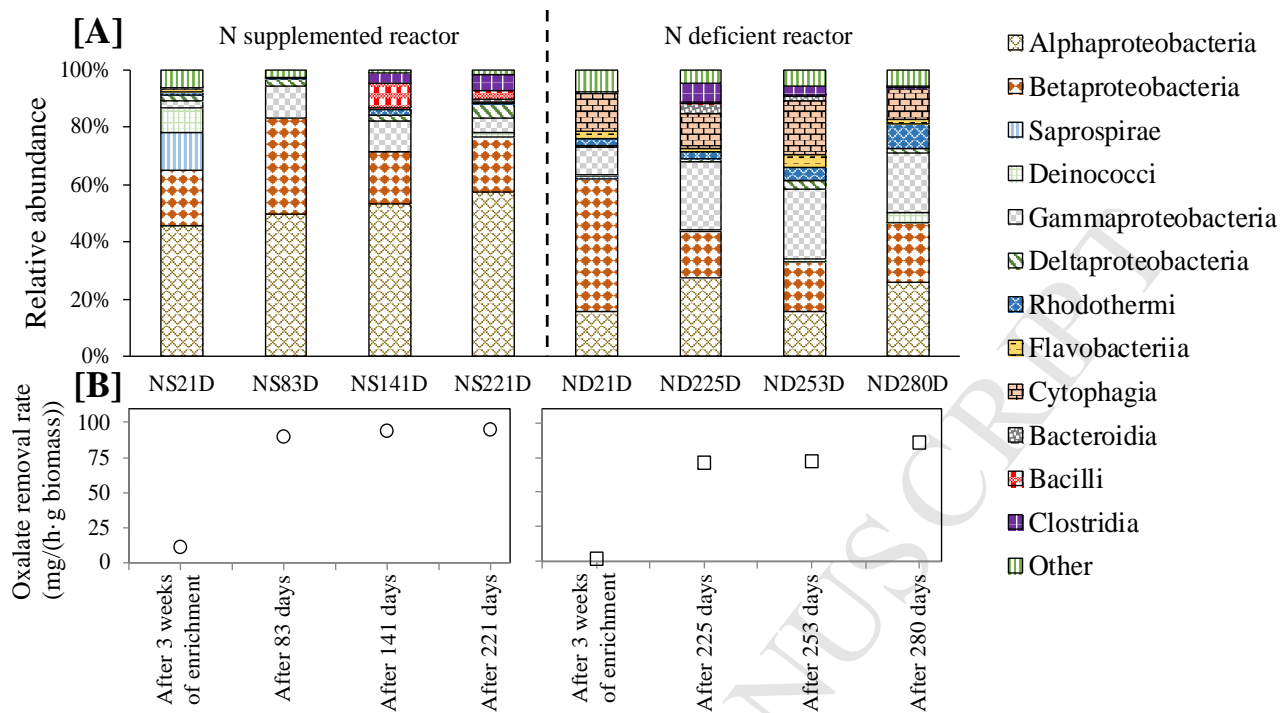
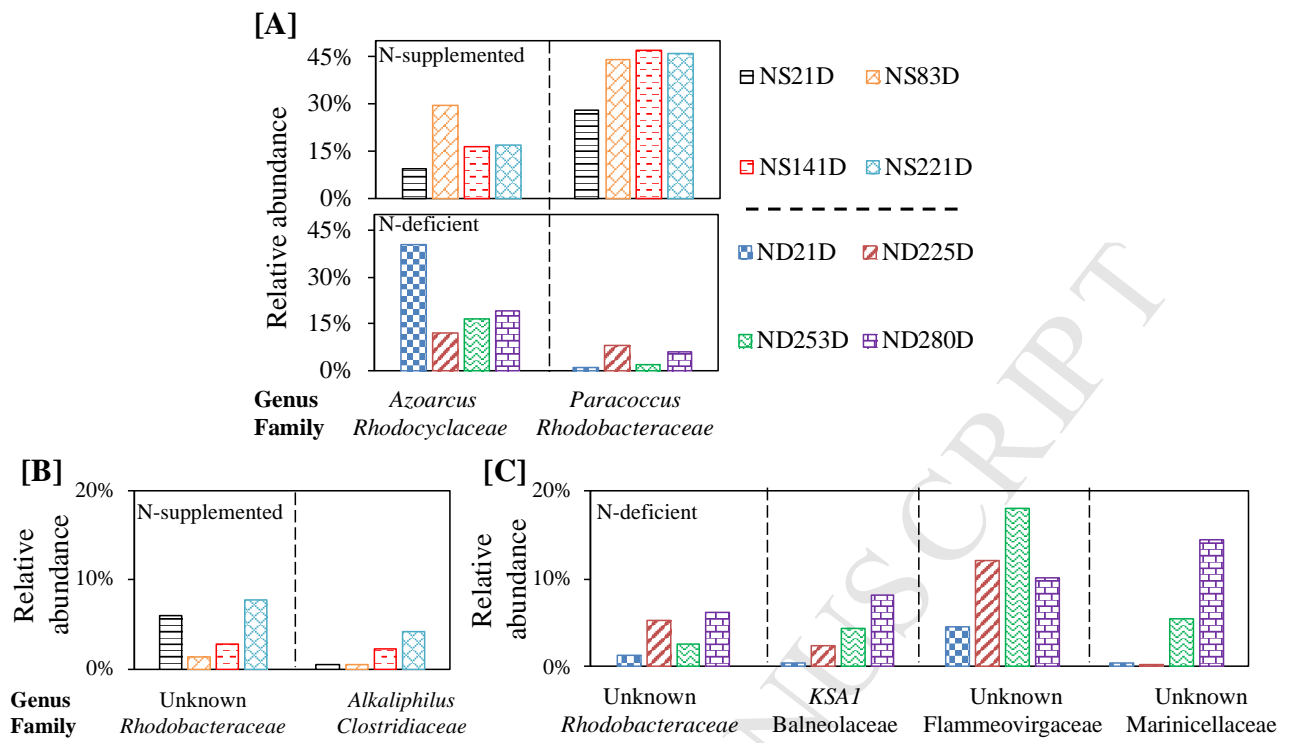


Fig. 7.



**Highlights**

- A first kinetic study on oxalate degradation under nitrogen (N) deficient conditions.
- The oxalate degradation kinetics of two haloalkaliphilic biofilms were compared.
- The N-deficient biofilm could degrade oxalate faster than the N-supplemented biofilm.
- The N-deficient culture had a higher affinity towards oxalate than N-supplemented.
- The microbial communities of the two biofilms were significantly different.